World in a mirror

9

A detour of a thousand pages starts with a single misstep.
Chairman Miaw

Dynamical systems often come equipped with discrete symmetries, such as the reflection symmetries of various potentials. As we shall show here and in Chapter **??**, symmetries simplify the dynamics in a rather beautiful way: If dynamics is invariant under a set of discrete symmetries G, the state space $\mathcal{M}$ is *tiled* by a set of symmetry-related tiles, and the dynamics can be reduced to dynamics within one such tile, the *fundamental domain* $\mathcal{M}/G$. If the symmetry is continuous the dynamics is reduced to a lower-dimensional desymmetrized system $\mathcal{M}/G$, with “ignorable” coordinates eliminated (but not forgotten). In either case families of symmetry-related full state space cycles are replaced by fewer and often much shorter “relative” cycles. In presence of a symmetry the notion of a prime periodic orbit has to be reexamined: it is replaced by the notion of a *relative periodic orbit*, the shortest segment of the full state space cycle which tiles the cycle under the action of the group. Furthermore, the group operations that relate distinct tiles do double duty as letters of an alphabet which assigns symbolic itineraries to trajectories.

Some familiarity with basic group-theoretic notions is assumed, with definitions relegated to Appendix C.1. We work out two examples commonly encountered in physical settings, $C_2 = D_1$ and $C_{3v} = D_3$ symmetries.

This chapter sets the stage for the factorization of spectral determinants to be undertaken in Chapter **??**.

9.1 Discrete symmetries

We show that a symmetry equates multiplets of equivalent orbits.

We start by defining a finite (discrete) group, its state space representations, and what we mean by a *symmetry* (*invariance*, *equivariance*) of a dynamical system.

Definition: A **finite group** consists of a set of elements

$$G = \{e, g_2, \ldots, g_{|G|}\} \tag{9.1}$$

and a group multiplication rule $g_j \circ g_i$ (often abbreviated as $g_j g_i$), satisfying

(1) If $g_i, g_j \in G$, then $g_j \circ g_i \in G$
(2) Associativity: $g_k \circ (g_j \circ g_i) = (g_k \circ g_j) \circ g_i$
(3) Identity e: $g \circ e = e \circ g = g$ for all $g \in G$
(4) Inverse g^{-1}: For every $g \in G$, there exists a unique element $h = g^{-1} \in G$ such that $h \circ g = g \circ h = e$.

$|G|$, the number of elements, is called the *order* of the group.

Definition: Coordinate transformations. An *active* linear coordinate transformation corresponds to a non-singular $[d\times d]$ matrix $\mathbf{T}$ that shifts the vector $x \in \mathcal{M}$ into another vector $\mathbf{T}x \in \mathcal{M}$

$$x \to \mathbf{T}x\,.$$

The corresponding *passive* coordinate transformation changes the coordinate system with respect to which the vector $f(x) \in \mathcal{M}$ is measured:

$$f(x) \to \mathbf{T}^{-1}f(x)$$

Together, a passive and active coordinate transformations yield the map in the transformed coordinates:

$$\hat{f}(x) = \mathbf{T}^{-1}f(\mathbf{T}x)\,. \tag{9.2}$$

Linear action of a discrete group G element g on states $x \in \mathcal{M}$ is given by a finite non-singular $[d\times d]$ matrix $\mathbf{g}$, the linear *representation* of element $g \in G$. In what follows we shall indicate by bold face $\mathbf{g}$ the matrix representation of the action of group element $g \in G$ on the state space vectors $x \in \mathcal{M}$.

If the coordinate transformation $\mathbf{g}$ belongs to a linear non-singular representation of a discrete (finite) group G, for any element $g \in G$, there exists a number $m \leq |G|$ such that

$$g^m \equiv \underbrace{g \circ g \circ \ldots \circ g}_{m \text{ times}} = e \quad \to \quad |\det \mathbf{g}| = 1\,. \tag{9.3}$$

Thus $\det\mathbf{g}$ is the mth root of 1, and the modulus of its determinant is unity.

Definition: Symmetry of a dynamical system. A dynamical system $(\mathcal{M}, f)$ is invariant under a symmetry group G if the "equations of motion" $f : \mathcal{M} \to \mathcal{M}$ (a discrete time map f, or the continuous flow f^t) from the d-dimensional manifold $\mathcal{M}$ into itself commute with all actions of G,

$$f(\mathbf{g}x) = \mathbf{g}f(x)\,. \tag{9.4}$$

Another way to state this is that the "law of motion" is invariant, i.e., retains its form in any symmetry-group related coordinate frame (9.2), and the dynamics is said to be *invariant* or *equivariant*

$$f(x) = \mathbf{g}^{-1}f(\mathbf{g}x) \tag{9.5}$$

for *any* state $x \in \mathcal{M}$ and *any* finite non-singular $[d \times d]$ matrix representation $\mathbf{g}$ of element $g \in G$.

For a generic ergodic orbit $f^t(x)$ the trajectory and any of its images under action of $g \in G$ are distinct with probability one, $f^t(x) \cap \mathbf{g} f^{t'}(x) = \emptyset$ for all t, t'.

For compact invariant sets, such as fixed points and periodic orbits, especially the short ones, the situation is very different.

Cycle multiplicities. If $g \in G$ is a symmetry of the dynamical problem, intrinsic properties of an equilibrium (Floquet exponents) or a cycle p (period, Floquet multipliers) and its image under a symmetry transformation g are equal. The multiplicity of a set of symmetry equivalent equilibria or cycles (topologically distinct, but mapped into each other by symmetry transformations) depends on the symmetry of a given equilibrium or cycle. Associated with a given equilibrium or cycle p is a maximal *isotropy* subgroup $G_p \subseteq G$, $G_p = \{e, b_2, b_3, \ldots, b_h\}$ of order $h = |G_p|$, whose elements leave the equilibrium or cycle p invariant. The elements of the coset space $g \in G/G_p$ generate the copies of p, so the multiplicity of an equilibrium or a cycle p is $m_p = |G|/|G_p|$.

Our labeling convention is usually lexical, i.e., we label a cycle by the cycle point whose label has the lowest value, and we label a class of degenerate cycles by the one with the lowest label $\hat{p}$. In what follows we shall drop the hat in $\hat{p}$ when it is clear from the context that we are dealing with symmetry distinct classes of cycles.

We take note three types of equilibria or cycles: asymmetric a, symmetric equilibria or cycles s built by repeats of relative cycles $\tilde{s}$, and boundary equilibria.

Asymmetric cycles: An equilibrium or periodic orbit is not symmetric if $\{x_a\} \cap \{\mathbf{g} x_a\} = \emptyset$, where $\{x_a\}$ is the set of periodic points belonging to the cycle a. Thus $g \in G$ generate $|G|$ distinct orbits with the same number of points and the same stability properties.

Symmetric cycles: A cycle s is *symmetric* (or *self-dual*) if operating with $g \in G_p \subseteq G$ on the set of cycle points reproduces the set. $g \in G_p$ acts a shift in time, advancing the cycle point by $f^{T_p/|G_p|}(ssp_s)$

Boundary equilibria: An equilibrium x_q lies on the boundary of domains related by action of the symmetry group if $\mathbf{g} x_q = x_q$ for all $g \in G$. A cycle $\{x_a\}$ that is pointwise invariant under all group operations lies in the “null-space” of the group action, and has multiplicity 1.

A string of unmotivated definitions (or an unmotivated definition of strings) has a way of making trite mysterious, so let’s switch gears: develop a feeling for why they are needed by first working out the simplest, 1-d example with a single reflection symmetry.

Example 9.1 Group D_1 - a reflection symmetric $1d$ map:

Consider a $1d$ map f with reflection symmetry $f(-x) = -f(x)$. An example is the bimodal “sawtooth” map of Fig. 9.1, piecewise-linear on the state space $\mathcal{M} = [-1, 1]$ split into three regions $\mathcal{M} = \{\mathcal{M}_L, \mathcal{M}_C, \mathcal{M}_R\}$ which we label with a 3-letter alphabet L(eft), C(enter), and R(ight). The symbolic dynamics is complete ternary dynamics, with any sequence of letters $\mathcal{A} = \{L, C, R\}$

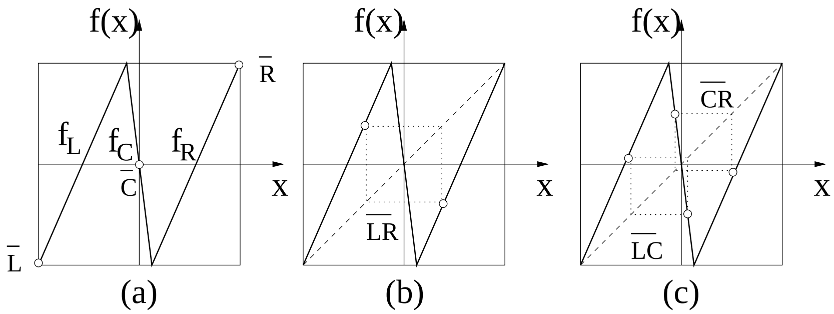

Fig. 9.1 The bimodal Ulam sawtooth map with the D_1 symmetry $f(-x) = -f(x)$. (a) Boundary fixed point $\overline{C}$, asymmetric fixed points pair $\{\overline{L}, \overline{R}\}$. (b) Symmetric 2-cycle $\overline{LR}$. (c) Asymmetric 2-cycles pair $\{\overline{LC}, \overline{CR}\}$. Continued in Fig. 9.6. (Yue-heng Lan)

corresponding to an admissible trajectory. Denote the reflection operation by $Rx = -x$. The 2-element group $\{e, R\}$ goes by many names - here we shall refer to it as C_2, the group of rotations in the plane by angle π, or D_1, dihedral group with a single reflection. The symmetry invariance of the map implies that if $\{x_n\}$ is a trajectory, than also $\{Rx_n\}$ is a trajectory because $Rx_{n+1} = Rf(x_n) = f(Rx_n)$.

Asymmetric cycles: R generates a reflection of the orbit with the same number of points and the same stability properties, see Fig. 9.1 (c).

Symmetric cycles: A cycle s is *symmetric* (or *self-dual*) if operating with R on the set of cycle points reproduces the set. The period of a symmetric cycle is even ($n_s = 2n_{\tilde{s}}$), and the mirror image of the x_s cycle point is reached by traversing the irreducible segment $\tilde{s}$ (relative periodic orbit) of length $n_{\tilde{s}}$, $f^{n_{\tilde{s}}}(x_s) = Rx_s$, see Fig. 9.1 (b).

Boundary cycles: In the example at hand there is only one cycle which is neither symmetric nor antisymmetric, but lies on the boundary: the fixed point $\overline{C}$ at the origin.

We shall continue analysis of this system in Example 9.4, and work out the symbolic dynamics of such reflection symmetric systems in Example 11.2.

As reflection symmetry is the only discrete symmetry that a map of the interval can have, this example completes the group-theoretic analysis of 1–d maps. For 3–d flows three discrete symmetry groups of order 2 are possible:

$$
\begin{aligned}
\text{reflection: } \sigma(x,y,z) &= (x,y,-z) \\
\text{rotation: } R(x,y,z) &= (-x,-y,z) \\
\text{inversion: } P(x,y,z) &=
\end{aligned}
\tag{9.6}
$$

Remark 9.5.1

Example 9.2 D_1 **desymmetrization of the Lorenz flow:**

Edward Lorenz arrived at the Lorenz equation

$$
\dot{x} = v(x) = \begin{bmatrix} \dot{x} \\ \dot{y} \\ \dot{z} \end{bmatrix} = \begin{bmatrix} \sigma(y-x) \\ \rho x - y - xz \\ xy - bz \end{bmatrix} \tag{9.7}
$$

by a drastic simplification of the Raleigh-Benard flow [17]. Lorenz fixed $\sigma = 10$, $b = 8/3$, and varied the "Rayleigh number" ρ.

Lorenz equation (9.7) is invariant under $[x,y]$-plane π rotation R:

$$
(x,y,z) \to R(x,y,z) = (-x,-y,z) \, . \tag{9.8}
$$

For “Rayleigh number” $0 < \rho < 1$ the origin equilibrium q_0 is attractive. At $\rho = 1$ equilibrium q_0 undergoes a pitchfork bifurcation into a R-symmetric pair of equilibria at

$$q_{1,2} = (\pm\sqrt{b(\rho-1)}, \pm\sqrt{b(\rho-1)}, \rho-1)\,, \tag{9.9}$$

with eigenvalues of the three equilibria given by:

$$\begin{aligned} q_0 \quad &: \quad (\lambda_+, \lambda_-, \lambda_s) = (-(\sigma+1)/2 \pm \sqrt{(\sigma-1)^2/4 + (\rho-1)\sigma}, -b) \\ q_{1,2} \quad &: \quad \text{roots of } \lambda^3 + \lambda^2(\sigma+b+1) + \lambda b(\sigma+\rho) + 2\sigma b(\rho-1) = 0\,. \end{aligned} \tag{9.10}$$

The q_0 $1d$ unstable manifold closes into a homoclinic orbit at $\rho = 13.56\ldots$. Beyond that, an infinity of associated periodic orbits are generated, until $\rho = 24.74\ldots$, where $q_{1,2}$ undergo a Hopf bifurcation. For $\rho > 24.74$ $q_{1,2}$ have one stable real eigenvalue, and one unstable complex conjugate pair as solutions to (9.10), leading to a spiral-out instability.

The flow is volume contracting (4.36):

$$\partial_i v_i = \sum_{i=1}^{3} \lambda_i(x,t) = -\sigma - b - 1 \tag{9.11}$$

at a constant, coordinate- and ρ-independent rate, set by Lorenz to $\partial_i v_i = -13.66\ldots$. As for periodic orbits and for long time averages there is no contraction / expansion along the flow, $\lambda_\| = 0$, and the sum of λ_i is constant by (9.11), there is only one independent λ_i to compute.

The action of the dihedral group D_1 generator R (9.8) on the Lorenz flow vector space $\mathcal{M} = \mathbb{R}^3$ is a rotation by π about the z-axis. R invariance decomposes the space into two irreducible subspaces $\mathcal{M} = \mathcal{M}^+ \oplus \mathcal{M}^-$, the z-axis $\mathcal{M}^+$ and the $[x, y]$ plane $\mathcal{M}^-$. The projection operators onto these two subspaces are

$$P^+ = \frac{1}{2}(1+R) = \begin{pmatrix} 0 & 0 & 0 \\ 0 & 0 & 0 \\ 0 & 0 & 1 \end{pmatrix}, \quad P^- = \frac{1}{2}(1-R) = \begin{pmatrix} 1 & 0 & 0 \\ 0 & 1 & 0 \\ 0 & 0 & 0 \end{pmatrix}. \tag{9.12}$$

The $1d$ $\mathcal{M}^+$ subspace is flow-invariant, with the full state space Lorenz equation (9.7) reduced to the exponential contraction to the q_0 equilibrium,

$$\dot{z} = -bz\,,$$

which is the reason why you never see this decomposition discussed in literature. Even though this subspace is so trivial, it plays important role as a topological obstruction, with the number of winds of a trajectory around it providing a natural symbolic dynamics. For flows in higher-dimensional state spaces the flow-invariant $\mathcal{M}^+$ subspace can be itself high-dimensional, with interesting dynamics.

The $\mathcal{M}^-$ subspace is *not* flow-invariant - the nonlinear terms the Lorenz equation (9.7) send initial conditions within $\mathcal{M}^-$ into the whole $\mathcal{M}$ - but R symmetry is nevertheless very useful. By defining a Poincaré section $\mathcal{P}$ to be any plane containing the z axis, the state space is divided into a half-space fundamental domain $\tilde{\mathcal{M}}$ and its 180^o rotation $R\tilde{\mathcal{M}}$. Then the dynamics can be reduced to fundamental domain, with any trajectory that pierces $\mathcal{P}$ reinjected through a 180^o rotation. Full space pairs p, Rp map into a single cycles $\tilde{p}$ in the fundamental domain, and any self-dual cycle $p = Rp = \tilde{p}R\tilde{p}$ is a repeat of a relative periodic orbit $\tilde{p}$.

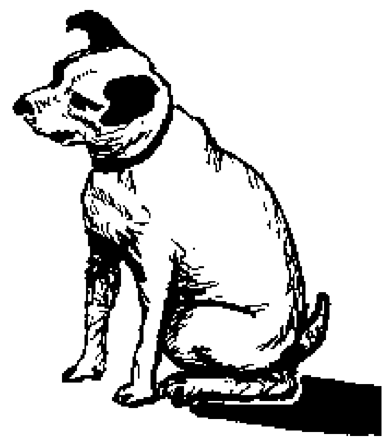

Fig. 9.2 The equilibria of the Lorenz flow for $\sigma = 10, b = 8/3, \rho = 28$. The stable eigenvector $\mathbf{e}^{(1)}$ of q_0 lies in the $\mathcal{M}^+ = z$-axis invariant subspace, while the unstable, R-rotation related eigenvector pair $\mathbf{e}^{(2,3)} \in \mathcal{M}^-$ is heteroclinic to $q_{1,2}$ equilibria. The R-rotation related $q_{1,2}$ equilibria have one stable real eigenvalue, and a complex conjugate pair which is unstable for $\rho > 24.74$.

9.7, page 124

9.7, page 124

9.8, page 124

We now turn to discussion of a general discrete symmetry group, with elements that do not commute, and illustrate it by the 3-disk game of pinball, Example 9.3 and Example 9.5.

in depth:
Appendix 23, p. 333

9.2 Relative periodic orbits

We show that a symmetry reduces computation of periodic orbits to repeats of shorter, "relative periodic orbit" segments.

Invariance of a flow under a symmetry means that the symmetric image of a cycle is again a cycle, with the same period and stability. The new orbit may be topologically distinct (in which case it contributes to the multiplicity of the cycle) or it may be the same cycle.

A cycle is *symmetric* under symmetry operation g if g acts on it as a shift in time, advancing the starting point to the starting point of a symmetry related segment. A symmetric cycle p can thus be subdivided into m_p repeats of a *irreducible segment*, "prime" in the sense that the full state space cycle is a repeat of it. Thus in presence of a symmetry the notion of a periodic orbit is replaced by the notion of the shortest segment of the full state space cycle which tiles the cycle under the action of the group. In what follows we refer to this segment as a *relative periodic orbit*.

Relative periodic orbits (or *equvariant periodic orbits*) are orbits $x(t)$ in state space $\mathcal{M}$ which exactly recur

$$x(t) = \mathbf{g}\, x(t+T) \tag{9.13}$$

for a fixed *relative period* T and a fixed group action $g \in G$. This group action is referred to as a "phase," or a "shift." For a discrete group by (9.3) $g^m = e$ for some finite m, so the corresponding full state space orbit is periodic with period mT.

The period of the full orbit is given by the $m_p \times$ (period of the relative periodic orbit), and the Floquet multiplier $\Lambda_{p,i}$ is given by $\Lambda_{\tilde{p},i}^{m_p}$ of the relative periodic orbit. The elements of the quotient space $b \in G/G_p$ generate the copies bp, so the multiplicity of the full state space cycle p is $m_p = |G| n_{\tilde{p}}/n_p$.

We now illustrate these ideas with the example of Section 1.3, symmetries of a 3-disk game of pinball.

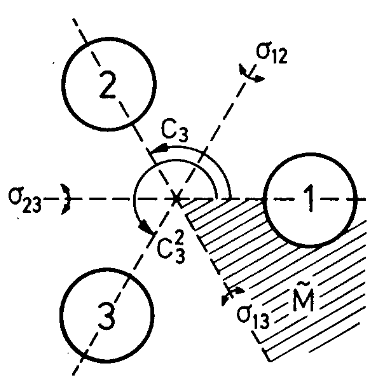

Fig. 9.3 The symmetries of three disks on an equilateral triangle. The fundamental domain is indicated by the shaded wedge.

Example 9.3 $C_{3v} = D_3$ invariance - 3-disk game of pinball:
As the three disks in Fig. 9.3 are equidistantly spaced, our game of pinball has a sixfold symmetry. The symmetry group of relabeling the 3 disks is the permutation group S_3; however, it is more instructive to think of this group geometrically, as C_{3v} (dihedral group D_3), the group of order $|G| = 6$ consisting of the identity element e, three reflections across axes $\{\sigma_{12}, \sigma_{23}, \sigma_{13}\}$, and two rotations by $2\pi/3$ and $4\pi/3$ denoted $\{C_3, C_3^2\}$. Applying an element (identity, rotation by $\pm 2\pi/3$, or one of the three possible reflections) of

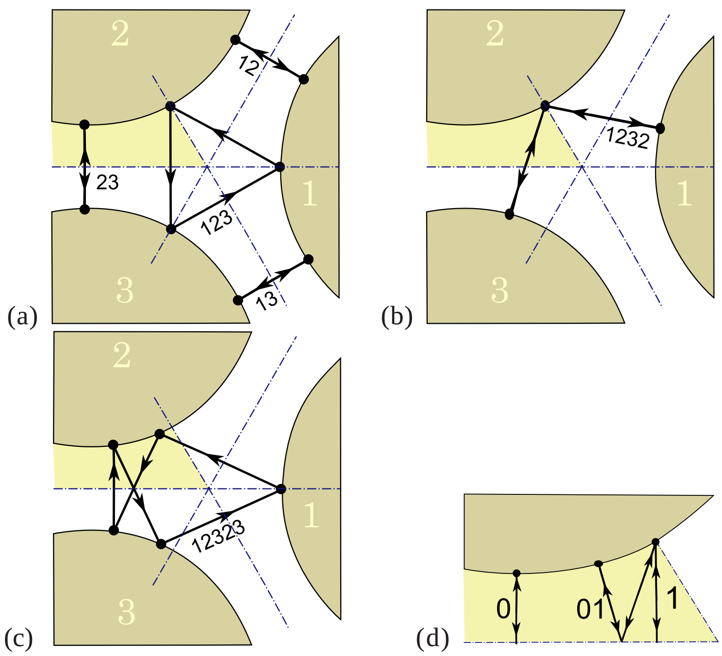

Fig. 9.4 The 3-disk pinball cycles: (a) $\overline{12}$, $\overline{13}$, $\overline{23}$, $\overline{123}$. Cycle $\overline{132}$ turns clockwise. (b) Cycle $\overline{1232}$; the symmetry related $\overline{1213}$ and $\overline{1323}$ not drawn. (c) $\overline{12323}$; $\overline{12123}$, $\overline{12132}$, $\overline{12313}$, $\overline{13131}$ and $\overline{13232}$ not drawn. (d) The fundamental domain, i.e., the 1/6th wedge indicated in (a), consisting of a section of a disk, two segments of symmetry axes acting as straight mirror walls, and the escape gap to the left. The above 14 full-space cycles restricted to the fundamental domain reduced to the two fixed points $\overline{0}$, $\overline{1}$, 2-cycle $\overline{10}$, and 5-cycle $\overline{00111}$ (not drawn).

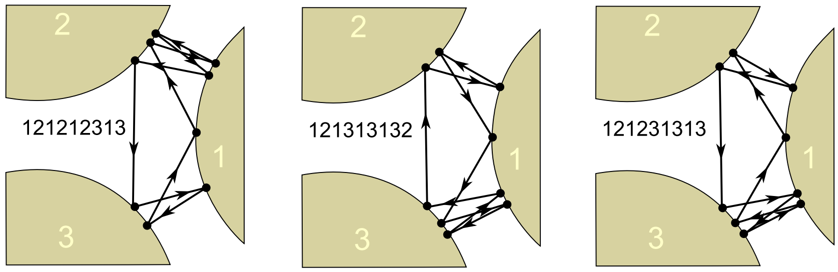

Fig. 9.5 Cycle $\overline{121212313}$ has multiplicity 6; shown here is $\overline{121313132} = \sigma_{23}\overline{121212313}$. However, $\overline{121231313}$ which has the same stability and period is related to $\overline{121313132}$ by time reversal, but not by any C_{3v} symmetry.

this symmetry group to a trajectory yields another trajectory. For instance, σ_{12}, the flip across the symmetry axis going through disk 1 interchanges the symbols 2 and 3; it maps the cycle $\overline{12123}$ into $\overline{13132}$, Fig. 9.5 (a). Cycles $\overline{12}$, $\overline{23}$, and $\overline{13}$ in Fig. 9.3 (a) are related to each other by rotation by $\pm 2\pi/3$, or, equivalently, by a relabeling of the disks.

9.6, page 123

The subgroups of D_3 are $D_1 = \{e, \sigma\}$, consisting of the identity and any one of the reflections, of order 2, and $C_3 = \{e, C_3, C_3^2\}$, of order 3, so possible cycle multiplicities are $|G|/|G_p| = 2$, 3 or 6.

The C_3 subgroup $G_p = \{e, C_3, C_3^2\}$ invariance is exemplified by 2 cycles $\overline{123}$ and $\overline{132}$ which are invariant under rotations by $2\pi/3$ and $4\pi/3$, but are mapped into each other by any reflection, Fig. 9.5 (b), and the multiplicity is $|G|/|G_p| = 2$.

The C_v type of a subgroup is exemplified by the invariances of $\hat{p} = 1213$. This cycle is invariant under reflection $\sigma_{23}\{\overline{1213}\} = \overline{1312} = \overline{1213}$, so the invariant subgroup is $G_{\hat{p}} = \{e, \sigma_{23}\}$, with multiplicity is $m_{\hat{p}} = |G|/|G_p| = 3$; the cycles in this class, $\overline{1213}$, $\overline{1232}$ and $\overline{1323}$, are related by $2\pi/3$ rotations, Fig. 9.5 (c).

A cycle of no symmetry, such as $\overline{12123}$, has $G_p = \{e\}$ and contributes in all six copies (the remaining cycles in the class are $\overline{12132}$, $\overline{12313}$, $\overline{12323}$, $\overline{13132}$ and $\overline{13232}$), Fig. 9.5 (a).

Besides the above discrete symmetries, for Hamiltonian systems cycles may be related by time reversal symmetry. An example are the cycles $\overline{121212313}$ and $\overline{121212323} = \overline{313212121}$ which have the same periods and stabilities, but are related by no space symmetry, see Fig. 9.5 (d). Continued in Example 9.5.

9.3 Domain for fundamentalists

So far we have used symmetry to effect a reduction in the number of independent cycles in cycle expansions. The next step achieves much more:

(1) Discrete symmetries can be used to restrict all computations to a *fundamental domain*, the $\mathcal{M}/G$ quotiented subspace of the full state space $\mathcal{M}$.

(2) Discrete symmetry tessellates the state space into copies of a fundamental domain, and thus induces a natural partition of state space. The state space is completely tiled by a fundamental domain and its symmetric images.

(3) Cycle multiplicities induced by the symmetry are removed by

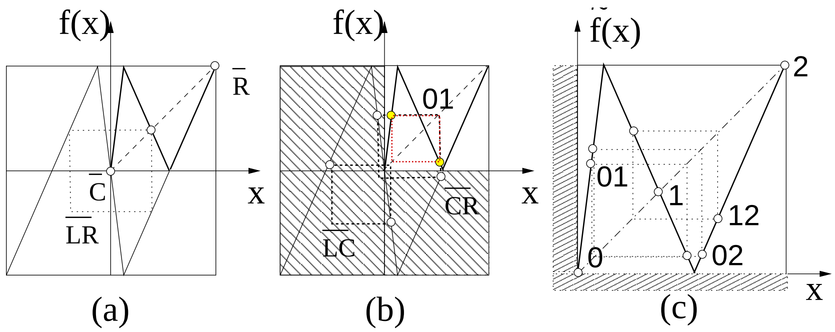

Fig. 9.6 The bimodal Ulam sawtooth map of Fig. 9.1 restricted to the $x \geq 0$ fundamental domain. $f(x)$ is indicated by thin line, and the fundamental domain map $\tilde{f}(\tilde{x})$ by thick line. (a) Boundary fixed point $\overline{C}$ maps into the fixed point $\overline{0}$. The asymmetric fixed point pair $\{\overline{L},\overline{R}\}$ maps into the fixed point $\overline{2}$, and the full state space symmetric 2-cycle $\overline{LR}$ into the fixed point $\overline{1}$. (b) The asymmetric 2-cycle pair $\{\overline{LC},\overline{CR}\}$ maps into the 2-cycle $\overline{01}$. (c) All fundamental domain fixed points and 2-cycles.

desymmetrization, reduction of the full dynamics to the dynamics on a *fundamental domain*. Each symmetry-related set of global cycles p corresponds to precisely one fundamental domain (or relative) cycle $\tilde{p}$. Conversely, each fundamental domain cycle $\tilde{p}$ traces out a segment of the global cycle p, with the end point of the cycle $\tilde{p}$ mapped into the irreducible segment of p with the group element $h_{\tilde{p}}$. The relative periodic orbits in the full space, folded back into the fundamental domain, are periodic orbits.

(4) The group elements $G = \{e, g_2, \ldots, g_{|G|}\}$ which map the fundamental domain $\tilde{\mathcal{M}}$ into its copies $g\tilde{\mathcal{M}}$, serve also as letters of a symbolic dynamics alphabet.

If the dynamics is invariant under a discrete symmetry, the state space $\mathcal{M}$ can be completely tiled by the fundamental domain $\tilde{\mathcal{M}}$ and its images $\mathcal{M}_a = a\tilde{\mathcal{M}}$, $\mathcal{M}_b = b\tilde{\mathcal{M}}$, ... under the action of the symmetry group $G = \{e, a, b, \ldots\}$,

$$\mathcal{M} = \tilde{\mathcal{M}} \cup \mathcal{M}_a \cup \mathcal{M}_b \cdots \cup \mathcal{M}_{|G|} = \tilde{\mathcal{M}} \cup a\tilde{\mathcal{M}} \cup b\tilde{\mathcal{M}} \cdots . \qquad (9.14)$$

Now we can use the invariance condition (9.4) to move the starting point x into the fundamental domain $x = \mathbf{a}\tilde{x}$, and then use the relation $a^{-1}b = h^{-1}$ to also relate the endpoint y to its image in the fundamental domain. While the global trajectory runs over the full space $\mathcal{M}$, the restricted trajectory is brought back into the fundamental domain $\tilde{\mathcal{M}}$ any time it exits into an adjoining tile; the two trajectories are related by the symmetry operation h which maps the global endpoint into its fundamental domain image.

Example 9.4 Group D_1 and reduction to the fundamental domain.
Consider again the reflection-symmetric bimodal Ulam sawtooth map $f(-x) = -f(x)$ of Example 9.1, with symmetry group $D_1 = \{e, R\}$. The state space $\mathcal{M} = [-1, 1]$ can be tiled by half-line $\tilde{\mathcal{M}} = [0, 1]$, and $R\tilde{\mathcal{M}} = [-1, 0]$, its image under a reflection across $x = 0$ point. The dynamics can then be restricted to the *fundamental domain* $\tilde{x}_k \in \tilde{\mathcal{M}} = [0, 1]$; every time a trajectory leaves this interval, it is mapped back using R.
In Fig. 9.6 the fundamental domain map $\tilde{f}(\tilde{x})$ is obtained by reflecting $x < 0$ segments of the global map $f(x)$ into the upper right quadrant. $\tilde{f}$ is also

bimodal and piecewise-linear, with $\tilde{\mathcal{M}} = [0,1]$ split into three regions $\tilde{\mathcal{M}} = \{\tilde{\mathcal{M}}_0, \tilde{\mathcal{M}}_1, \tilde{\mathcal{M}}_2\}$ which we label with a 3-letter alphabet $\tilde{\mathcal{A}} = \{0,1,2\}$. The symbolic dynamics is again complete ternary dynamics, with any sequence of letters $\{0,1,2\}$ admissible.

However, the interpretation of the "desymmetrized" dynamics is quite different - the multiplicity of every periodic orbit is now 1, and relative periodic orbits of the full state space dynamics are all periodic orbits in the fundamental domain. Consider Fig. 9.6

In (a) the boundary fixed point $\overline{C}$ is also the fixed point $\overline{0}$. In this case the set of points invariant under group action of D_1, $\tilde{\mathcal{M}} \cap R\tilde{\mathcal{M}}$, is just this fixed point $x = 0$, the reflection symmetry point.

The asymmetric fixed point pair $\{\overline{L},\overline{R}\}$ is reduced to the fixed point $\overline{2}$, and the full state space symmetric 2-cycle $\overline{LR}$ is reduced to the fixed point $\overline{1}$. The asymmetric 2-cycle pair $\{\overline{LC},\overline{CR}\}$ is reduced to the 2-cycle $\overline{01}$. Finally, the symmetric 4-cycle $\overline{LCRC}$ is reduced to the 2-cycle $\overline{02}$. This completes the conversion from the full state space for all fundamental domain fixed points and 2-cycles, Fig. 9.6 (c).

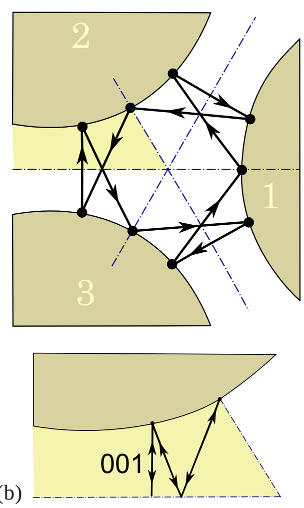

Fig. 9.7 (a) The pair of full-space 9-cycles, the counter-clockwise $\overline{121232313}$ and the clockwise $\overline{131323212}$ correspond to (b) one fundamental domain 3-cycle $\overline{001}$.

Example 9.5 3-disk game of pinball in the fundamental domain

If the dynamics is symmetric under interchanges of disks, the absolute disk labels $\epsilon_i = 1, 2, \cdots, N$ can be replaced by the symmetry-invariant relative disk→disk increments g_i, where g_i is the discrete group element that maps disk $i-1$ into disk i. For 3-disk system g_i is either reflection σ back to initial disk (symbol '0') or rotation by C to the next disk (symbol '1'). An immediate gain arising from symmetry invariant relabeling is that N-disk symbolic dynamics becomes $(N-1)$-nary, with no restrictions on the admissible sequences.

An irreducible segment corresponds to a periodic orbit in the *fundamental domain*, a one-sixth slice of the full 3-disk system, with the symmetry axes acting as reflecting mirrors (see Fig. 9.3(d)). A set of orbits related in the full space by discrete symmetries maps onto a single fundamental domain orbit. The reduction to the fundamental domain desymmetrizes the dynamics and removes all global discrete symmetry-induced degeneracies: rotationally symmetric global orbits (such as the 3-cycles $\overline{123}$ and $\overline{132}$) have multiplicity 2, reflection symmetric ones (such as the 2-cycles $\overline{12}$, $\overline{13}$ and $\overline{23}$) have multiplicity 3, and global orbits with no symmetry are 6-fold degenerate. Table 11.1 lists some of the shortest binary symbols strings, together with the corresponding full 3-disk symbol sequences and orbit symmetries. Some examples of such orbits are shown in Figs. 9.5 and 9.7. Continued in Example 11.3.

9.4 Continuous symmetries

What if the "law of motion" retains its form (9.5) in a family of coordinate frames $f(x) = \mathbf{g}^{-1} f(\mathbf{g}x)$ related by a group of *continuous* symmetries? The notion of "fundamental domain" is of no use here. Instead, as we shall see, continuous symmetries reduce dynamics to a desymmetrized system of lower dimensionality, by elimination of "ignorable" coordinates.

Definition: A Lie group is a topological group G such that (1) G has the structure of a smooth differential manifold. (2) The composition map $G \times G \to G : (g, h) \to gh^{-1}$ is smooth. By "smooth" in this text we always mean $\mathbb{C}^\infty$ differentiable. If you are mystified by the above definition, don't be. Just think "aha, like the rotation group $SO(3)$?"

If action of every element g of a group G commutes with the flow $\dot{x} = v(x)$, $x(t) = f^t(x_0)$,

$$\mathbf{g}v(x) = v(\mathbf{g}x) \,, \qquad \mathbf{g}f^t(x_0) = f^t(\mathbf{g}x_0) \,, \tag{9.15}$$

the dynamics is said to be *invariant* or *equivariant* under G.

Let G be a group, $\mathcal{M}$ a set, and $g\mathcal{M} \longrightarrow \mathcal{M}$ a group action. For any $x \in \mathcal{M}$, the *orbit* $\mathcal{M}(x)$ of x is the set of all group actions

$$\mathcal{M}(x) = \{\mathbf{g}\, x \mid g \in G\} \subset \mathcal{M} \,.$$

For a given state space point x the group of N continuous transformations together with the time translation sweeps out a smooth (N+1)-dimensional manifold of equivalent orbits. The time evolution itself is a noncompact 1-parameter Lie group; however, for solutions p for which the N-dimensional group manifold is periodic in time T_p, the orbit of x_p is a *compact* invariant manifold $\mathcal{M}_p$. The simplest example is the $N = 0$ case, where the invariant manifold $\mathcal{M}_p$ is the $1d$-torus traced out by the periodic trajectory. Thus all continuous symmetries can be considered on the same footing, and the closure of the set of comapact unstable invariant manifolds $\mathcal{M}_p$ is the non-wandering set Ω of dynamics in presence of a continuous global symmetry (see Section 2.1.1).

The desymmetrized state space is the quotient space $\mathcal{M}/G$. The reduction to $\mathcal{M}/G$ amounts to a change of coordinates where the "ignorable angles" $\{t, \theta_1, \cdots, \theta_N\}$ parametrize N+1 time and group translations can be separated out. A simple example is the "rectification" of the harmonic oscillator by a change to polar coordinates, Example 6.1.

9.4.1 Lie groups for pedestrians

All the group theory that you shall need here is in principle contained in the *Peter-Weyl theorem*, and its corollaries: A compact Lie group G is completely reducible, its representations are fully reducible, every compact Lie group is a closed subgroup of $U(n)$ for some n, and every continuous, unitary, irreducible representation of a compact Lie group is finite dimensional.

Instead of writing yet another tome on group theory, in what follows we serve group theoretic nuggets on need-to-know basis, following a well-trod pedestrian route through a series of examples of familiar bits of group theory and Fourier analysis (but take a modicum of high, cyclist road in the text proper).

Consider infinitesimal transformations of form $g = 1 + iD$, $|D^a_b| \ll 1$, i.e., the transformations connected to the identity (in general, we also need to combine this with effects of invariance under discrete coordinate transformations, already discussed above). *Unitary* transformations $\exp(i\theta_j T_j)$ are generated by sequences of infinitesimal transformations of form

$$g_a{}^b \simeq \delta^a_b + i\delta\theta_i (T_i)^b_a \qquad gSpace \in \mathbb{R}^N\,, \quad T_i \text{ hermitian}\,.$$

where T_i, the *generators* of infinitesimal transformations, are a set of linearly independent $[d\times d]$ hermitian matrices. In terms of the generators T_i, a tensor $h_{ab\ldots}{}^{\cdots c}$ is invariant if T_i "annihilate" it, i.e., $T_i \cdot h = 0$:

$$(T_i)_a^{a'} h_{a'b\ldots}{}^{c\ldots} + (T_i)_b^{b'} h_{ab'\ldots}{}^{c\ldots} - (T_i)_{c'}^{c} h_{ab\ldots}{}^{c'\cdots} + \ldots = 0\,. \tag{9.16}$$

Example 9.6 Lie algebra.

As one does not want the symmetry rules to change at every step, the generators T_i, $i = 1, 2, \ldots, N$, are themselves invariant tensors:

$$(T_i)\,{}^a_b = g^a{}_{a'} g_b{}^{b'} g_{ii'}\,(T_{i'})\,{}^{a'}_{b'}\,, \tag{9.17}$$

where $g_{ij} = \left[e^{-i\theta_k C_k}\right]_{ij}$ is the adjoint $[N \times N]$ matrix representation of $g \in \mathcal{G}$. The $[d\times d]$ matrices T_i are in general non-commuting, and from (9.16) it follows that they close N-element *Lie algebra*

$$T_i T_j - T_j T_i = i C_{ijk} T_k \qquad i, j, k = 1, 2, ..., N\,,$$

where the fully antisymmetric adjoint representation generators $[C_k]_{ij} = C_{ijk}$ are known as the *structure constants.*

Example 9.7 Group $SO(2)$.

$SO(2)$ is the group of rotations in a plane, smoothly connected to the unit element (i.e. the inversion $x \to -x$ is excluded). A group element can be parameterized by angle θ, and its action on smooth periodic functions is generated by

$$g(\theta) = e^{i\theta\mathbf{T}}\,, \quad \mathbf{T} = -i\frac{d}{d\theta}\,,$$

$g(\theta)$ rotates a periodic function $u(\theta + 2\pi) = u(\theta)$ by θ mod 2π:

$$g(\theta)u(\theta') = u(\theta' + \theta)$$

The multiplication law is $g(\theta)g(\theta') = g(\theta+\theta')$. If the group G actions consists of N such rotations which commute, for example a N-dimensional box with periodic boundary conditions, the group G is an Abelian group that acts on a torus T^N.

9.4.2 Relative periodic orbits

Consider a flow invariant under a global continuous symmetry (Lie group) G. A relative periodic orbit p is an orbit in state space $\mathcal{M}$ which exactly recurs

$$x_p(t) = \mathbf{g}_p x_p(t + T_p)\,, \qquad x_p(t) \in \mathcal{M}_p \tag{9.18}$$

for a fixed *relative period* T_p and a fixed group action $g_p \in G_p \subset G$ that "rotates" the endpoint $x_p(T_p)$ back into the initial point $x_p(0)$. The group action g_p is referred to as a "phase," or a "shift."

Example 9.8 Continuous symmetries of the plane Couette flow.
The Navier-Stokes plane Couette flow defined as a flow between two countermoving planes, in a box periodic in stream-wise and span-wise directions, a relative periodic solution is a solution that recurs at time T_p with exactly the same disposition of velocity fields over the entire box, but shifted by a 2-dimensional (stream-wise,span-wise) translation g_p. The $SO(2) \times SO(2)$ continuous symmetry acts on a 2-torus T^2.

For dynamical systems with continuous symmetries parameters $\{t, \theta_1, \cdots, \theta_N\}$ are real numbers, π/θ_j are almost never rational, and relative periodic orbits are almost never eventually periodic. As almost any such orbit explores ergodically the manifold swept by action of $G \times t$, they are sometimes referred to as "quasiperiodic". However, a relative periodic orbit can be pre-periodic if it is invariant under a discrete symmetry: If $g^m = 1$ is of finite order m, then the corresponding orbit is periodic with period mT_p. If g is not of finite order k, the orbit is periodic only after the action of g, as in (9.18). In either discrete or continuous symmetry case, we refer to the orbits $\mathcal{M}_p$ in $\mathcal{M}$ satisfying (9.18) as *relative periodic orbits*. Morally, as it will be shown in Chapter **??**, they are the true "prime" orbits, i.e., the shortest segments that under action of G tile the entire invariant submanifolds $\mathcal{M}_p$.

9.5 Stability

A infinitesimal symmetry group transformation maps a trajectory in a nearby equivalent trajectory, so we expect the initial point perturbations along to group manifold to be marginal, with unit eigenvalue. The argument is akin to (4.7), the proof of marginality of perturbations along a periodic orbit. In presence of an N-dimensional Lie symmetry group G, further N eigenvalues equal unity. Consider two nearby initial points separated by an N-dimensional infinitesimal group transformation $\delta\theta$: $\delta x(0) = \mathbf{g}(\delta\theta)x_0 - x_0 = i\delta\theta \cdot \mathbf{T}x_0$. By the commutativity of the group with the flow, $\mathbf{g}(\delta\theta)f^t(x_0) = f^t(\mathbf{g}(\delta\theta)x_0)$. Expanding both sides, keeping the leading term in $\delta\theta$, and using the definition of the fundamental matrix (4.6), we observe that $J^t(x_0)$ transports the N-dimensional tangent vector frame at x_0 to the rotated tangent vector frame at $x(t)$ at time t:

$$\delta x(t) = \mathbf{g}(\theta, t) J^t(x_0)\, \delta x(0)\,. \tag{9.19}$$

For relative periodic orbits $\mathbf{g}_p x(T_p) = x(0)$, at any point along cycle p the group tangent vector $\mathbf{T}x(t)$ is an eigenvector of the fundamental matrix $J_p(x) = \mathbf{g}_p J^{T_p}(x)$ with an eigenvalue of unit magnitude,

$$J^{T_p}(x)\, x_0 = \mathbf{g}(\theta)\mathbf{T}x(t)\,, \qquad x \in p\,. \tag{9.20}$$

Two successive points along the cycle separated by $\delta x(0)$ have the same separation after a completed period $\delta x(T_p) = \mathbf{g}_p \delta x(0)$, hence eigenvalue of magnitude 1.

9.5.1 Boundary orbits

Peculiar effects arise for orbits that run on a symmetry lines that border a fundamental domain. The state space transformation $\mathbf{h} \neq \mathbf{e}$ leaves invariant sets of *boundary* points; for example, under reflection σ across a symmetry axis, the axis itself remains invariant. Some care need to be exercised in treating the invariant "boundary" set $\mathcal{M} = \tilde{\mathcal{M}} \cap \mathcal{M}_a \cap \mathcal{M}_b \cdots \cap \mathcal{M}_{|G|}$. The properties of boundary periodic orbits that belong to such point-wise invariant sets will require a bit of thinking.

In our 3-disk example, no such orbits are possible, but they exist in other systems, such as in the bounded region of the Hénon-Heiles potential (Remark 9.5.1) and in $1d$ maps of Example 9.1. For the symmetrical 4-disk billiard, there are in principle two kinds of such orbits, one kind bouncing back and forth between two diagonally opposed disks and the other kind moving along the other axis of reflection symmetry; the latter exists for bounded systems only. While for low-dimensional state spaces there are typically relatively few boundary orbits, they tend to be among the shortest orbits, and they play a key role in dynamics.

While such boundary orbits are invariant under some symmetry operations, their neighborhoods are not. This affects the fundamental matrix M_p of the orbit and its Floquet multipliers.

Here we have used a particularly simple direct product structure of a global symmetry that commutes with the flow to reduce the dynamics to a symmetry reduced $(d-1-N)$-dimensional state space $\mathcal{M}/G$.

Summary

In Section 2.1.1 we made a lame attempt to classify "all possible motions:" (1) equilibria, (2) periodic orbits, (3) everything else. Now one can discern in the fog of dynamics outline of a more serious classification - long time dynamics takes place on the closure of a set of all invariant compact sets preserved by the dynamics, and those are: (1) 0-dimensional equilibria $\mathcal{M}_q$, (2) 1-dimensional periodic orbits $\mathcal{M}_p$, (3) global symmetry induced N-dimensional relative equilibria $\mathcal{M}_{tw}$ (4) $(N$+1)-dimensional relative periodic orbits $\mathcal{M}_p$, (5) terra incognita. We have some inklings of the "terra incognita:" for example, symplectic symmetry induces existence of KAM-tori, and in general dynamical settings we are encountering more and more examples of *partially hyperbolic invariant tori*, isolated tori that are consequences of dynamics, not of a global symmetry, and which cannot be represented by a single relative periodic orbit, but require a numerical computation of full $(N$+1)-dimensional compact invariant sets and their infinite-dimensional linearized fundamental matrices, marginal in $(N$+1) dimensions, and hyperbolic in the rest.

The main result of this chapter can be stated as follows: If a dynamical system $(\mathcal{M}, f)$ has a symmetry G, the symmetry should be deployed to "quotient" the state space $\mathcal{M}/G$, i.e., identify all $x \in \mathcal{M}$ related by the symmetry.

(1) In presence of a discrete symmetry G, associated with each full state space cycle p is a maximal isotropy subgroup $G_p \subseteq G$ of order $1 \leq |G_p| \leq |G|$, whose elements leave p invariant. The isotropy subgroup G_p acts on p as time shift, tiling it with $|G_p|$ copies of its shortest invariant segment, the relative periodic orbit $\tilde{p}$. The elements of the coset $b \in G/G_p$ generate $m_p = |G|/|G_p|$ distinct copies of p.

This reduction to the fundamental domain $\tilde{\mathcal{M}} = \mathcal{M}/G$ simplifies symbolic dynamics and eliminates symmetry-induced degeneracies. For the short orbits the labor saving is dramatic. For example, for the 3-disk game of pinball there are 256 periodic points of length 8, but reduction to the fundamental domain non-degenerate prime cycles reduces the number of the distinct cycles of length 8 to 30.

Amusingly, in this extension of "periodic orbit" theory from unstable 1-dimensional closed orbits to unstable $(N+1)$-dimensional compact manifolds $\mathcal{M}_p$ invariant under continuous symmetries, there are either no or proportionally few periodic orbits. Likelihood of finding a periodic orbit is *zero*. One expects some only if in addition to a continuous symmetry one has a discrete symmetry, or the particular invariant compact manifold $\mathcal{M}_p$ is invariant under a discrete subgroup of the continuous symmetry. Relative periodic orbits are almost never eventually periodic, i.e., they almost never lie on periodic trajectories in the full state space, unless forced to do so by a discrete symmetry, so looking for periodic orbits in systems with continuous symmetries is a fool's errand.

Atypical as they are (no chaotic solution will be confined to these discrete subspaces) they are important for periodic orbit theory, as there the shortest orbits dominate.

We feel your pain, but trust us: once you grasp the relation between the full state space $\mathcal{M}$ and the desymmetrized G-quotiented $\mathcal{M}/G$, you will find the life as a fundamentalist so much simpler that you will never return to your full state space confused ways of yesteryear.

Further reading

Examples of systems with discrete symmetries. One has a D_1 symmetry in the Lorenz system [1, 2], the Ising model, and in the $3d$ anisotropic Kepler potential [**?**, **?**, **?**], a $D_3 = C_{3v}$ symmetry in Hénon-Heiles type potentials [3–6], a $D_4 = C_{4v}$ symmetry in quartic oscillators [7, 8], in the pure x^2y^2 potential [9, 10] and in hydrogen in a magnetic field [11], and a $D_2 = C_{2v} = C_2 \times C_2$ symmetry in the stadium billiard [12]. A very nice application of desymmetrization is carried out in Ref. [13].

Lorenz equation: The Lorenz equation (9.7) is the most celebrated early illustration of "deterministic chaos" [17] (but not the first - the honor goes to Dame Cartwright [31]). Lorenz's paper, which can be found in reprint collections Refs. [21, 22], is a pleasure to read, and is still one of the best introductions to the physics motivating such models. The equations, a set of ODEs in $\mathbb{R}^3$, exhibit strange attractors [18–20] whose geometry reflects the underlying symmetry of the ODEs. Lorenz truncation to 3 modes is so drastic that the model bears no relation to the physical hydrodynamics problem that motivated it. Frøyland [23] has a nice brief discussion of Lorenz flow. Frøyland and Alfsen [24] plot many periodic and heteroclinic orbits of the Lorenz flow; some of the symmetric ones are included in Ref. [23]. Guckenheimer-Williams [25] and Afraimovich-Bykov-Shilnikov [26] offer in-depth discussion of the Lorenz equation. The most detailed study of the Lorenz equation was undertaken by Sparrow [27]. For a physical interpretation of ρ as "Rayleigh number" see Jackson [28] and Seydel [29]. For a detailed pictures of Lorenz invariant manifolds consult Vol II of Jackson [28]. You will appreciate why `ChaosBook.org` starts out with the desymmetrized version - the Rössler flow - instead of the more traditional Lorenz. The discrete symmetry is not merely "a symmetry;" it also enforces miracles such as heteroclinic connections, with unstable manifolds of some equilibria flowing into stable manifolds of other equilibria. Miranda and Stone [32] were first to quotient the D_1 symmetry and explicitly construct the desymmetrized, "proto-Lorenz system," by a polynomial transformation into coordinates invariant under the action of the symmetry group [37]. Discussion of Exercise 9.8 follows Letellier and Gilmore [35], who interpret the proto-Lorentz and its "double cover" Lorenz as "intensities" being the squares of "amplitudes." For further discussions of the Lorenz D_1 symmetry see Refs. [**?**, 33].

Hénon-Heiles potential. An example of a system with C_{3v} symmetry is provided by the motion of a particle in the Hénon-Heiles potential [3]

$$V(r,\theta) = \frac{1}{2}r^2 + \frac{1}{3}r^3 \sin(3\theta) \ .$$

Our 3-disk coding is insufficient for this system because of the existence of elliptic islands and because the three orbits that run along the symmetry axis cannot be labeled in our code. As these orbits run along the boundary of the fundamental domain, they require the special treatment discussed in Section 9.5.1.

Cycles and symmetries. We conclude this section with a few comments about the role of symmetries in actual extraction of cycles. In the N-disk billiard example, a fundamental domain is a sliver of the N-disk configuration space delineated by a pair of adjoining symmetry axes. The flow may further be reduced to a return map on a Poincaré surface of section. While in principle any Poincaré surface of section will do, a natural choice in the present context are crossings of symmetry axes, see Example 7.6.

In actual numerical integrations only the last crossing of a symmetry line needs to be determined. The cycle is run in global coordinates and the group elements associated with the crossings of symmetry lines are recorded; integration is terminated when the orbit closes in the fundamental domain. Periodic orbits with non-trivial symmetry subgroups are particularly easy to find since their points lie on crossings of symmetry lines, see Example 7.6.

Exercises

(9.1) **3-disk fundamental domain symbolic dynamics.** Try to sketch $\overline{0}$, $\overline{1}$, $\overline{01}$, $\overline{001}$, $\overline{011}$, $\cdots$. in the fundamental domain, and interpret the symbols $\{0,1\}$ by relating them to topologically distinct types of collisions. Compare with Table 11.1. Then try to sketch the location of periodic points in the Poincaré section of the billiard flow. The point of this exercise is that while in the configuration space longer cycles look like a hopeless jumble, in the Poincaré section they are clearly and logically ordered. The Poincaré section is always to be preferred to projections of a flow onto the configuration space coordinates, or any other subset of state space coordinates which does not respect the topological organization of the flow.

(9.2) **Reduction of 3-disk symbolic dynamics to binary.**

(a) Verify that the 3-disk cycles
$\{\overline{1\,2}, \overline{1\,3}, \overline{2\,3}\}$, $\{\overline{1\,2\,3}, \overline{1\,3\,2}\}$, $\{\overline{12\,13}$ + 2 perms.$\}$,
$\{\overline{121\,232\,313}$ + 5 perms.$\}$, $\{\overline{121\,323}$+ 2 perms.$\}$,
$\cdots$,
correspond to the fundamental domain cycles
$\overline{0}$, $\overline{1}$, $\overline{01}$, $\overline{001}$, $\overline{011}$, $\cdots$ respectively.

(b) Check the reduction for short cycles in Table 11.1 by drawing them both in the full 3-disk system and in the fundamental domain, as in Fig. **??**.

(c) Optional: Can you see how the group elements listed in Table 11.1 relate irreducible segments to the fundamental domain periodic orbits?

(9.3) **Fundamental domain fixed points.** Use the formula (8.11) for billiard fundamental matrix to compute the periods T_p and the expanding eigenvalues Λ_p of the fundamental domain $\overline{0}$ (the 2-cycle of the complete 3-disk space) and $\overline{1}$ (the 3-cycle of the complete 3-disk space) fixed points:

	T_p	Λ_p
$\overline{0}$:	$R-2$	$R-1+R\sqrt{1-2/R}$
$\overline{1}$:	$R-\sqrt{3}$	$-\frac{2R}{\sqrt{3}}+1-\frac{2R}{\sqrt{3}}\sqrt{1-\sqrt{3}/R}$

(9.21)

We have set the disk radius to $a = 1$.

(9.4) **Fundamental domain 2-cycle.** Verify that for the $\overline{10}$-cycle the cycle length and the trace of the fundamental matrix are given by

$$\begin{aligned} L_{10} &= 2\sqrt{R^2-\sqrt{3}R+1}-2, \\ \mathrm{tr}\,\mathbf{J}_{10} &= \Lambda_{10}+1/\Lambda_{10} \\ &= 2L_{10}+2+\frac{1}{2}\frac{L_{10}(L_{10}+2)^2}{\sqrt{3}R/2-1} \end{aligned} \quad (9.22)$$

The $\overline{10}$-cycle is drawn in Fig. **??**. The unstable eigenvalue Λ_{10} follows from (4.20).

(9.5) **A test of your pinball simulator: $\overline{10}$-cycle.** Test your Exercise 8.3 pinball simulator stability evaluation by checking numerically the exact analytic $\overline{10}$-cycle stability formula (9.22).

(9.6) **The group C_{3v}.** We will compute a few of the properties of the group C_{3v}, the group of symmetries of an equilateral triangle

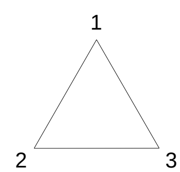

(a) For this exercise, get yourself a good textbook, a book like Hamermesh [16] or Tinkham [15], and read up on classes and characters. All discrete groups are isomorphic to a permutation group or one of its subgroups, and elements of the permutation group can be expressed as cycles. Express the elements of the group C_{3v} as cycles. For example, one of the rotations is (123), meaning that vertex 1 maps to 2 and 2 to 3 and 3 to 1.

(b) Find the subgroups of the group C_{3v}.

(c) Find the classes of C_{3v} and the number of elements in them.

(d) There are three irreducible representations for the group. Two are one dimensional and the other one of multiplicity 2 is formed by $[2\times 2]$ matrices of the form

$$\begin{bmatrix} \cos\theta & \sin\theta \\ -\sin\theta & \cos\theta \end{bmatrix}.$$

Find the matrices for all six group elements.

(e) Use your representation to find the character table for the group.

(9.7) **Lorenz system in polar coordinates.** Use (6.7), (6.8) to rewrite the Lorenz equation

$$\dot{x} = v(x) = \begin{bmatrix} \dot{x} \\ \dot{y} \\ \dot{z} \end{bmatrix} = \begin{bmatrix} \sigma(y-x) \\ \rho x - y - xz \\ xy - bz \end{bmatrix} \qquad (9.23)$$

in polar coordinates (r, θ, z), where $(x, y) = (r\cos\theta, r\sin\theta)$.

1. Show that in the polar coordinates Lorentz flow takes form

$$\begin{aligned} \dot{r} &= \frac{r}{2}(-\sigma - 1 + (\sigma + \rho - z)\sin 2\theta \\ &\quad +(1-\sigma)\cos 2\theta) \\ \dot{\theta} &= \frac{1}{2}(-\sigma + \rho - z - (\sigma+1)\sin 2\theta \\ &\quad +(\sigma + \rho - z)\cos 2\theta) \\ \dot{z} &= -bz + \frac{r^2}{2}\sin 2\theta\,. \end{aligned} \qquad (9.24)$$

2. Show that the transformation to polar coordinates is invertible almost everywhere. Where does the inverse not exist?
3. Show that (9.24) has two equilibria:

$$\begin{aligned} (r_0, z_0) &= (0, 0)\,, \qquad \theta_0 \text{ undefined} \\ (r_q, \theta_q, z_q) &= (\sqrt{2b(\rho-1)}, \frac{\pi}{4}, \rho - 1) \end{aligned} \qquad (9.25)$$

4. Compute eigenvalues and eigenvectors of the two equilibria. Compare with the equilibria of the Lorenz flow (see Example 9.2).
5. Plot the Lorenz strange attractor both in the original form (9.23) and in the polar coordinates (might look better if you expand the angle $\theta \in [0, \pi]$ to $2\theta \in [0, 2\pi]$) for the Lorenz parameter values $\sigma = 10$, $b = 8/3$, $\rho = 28$. Topologically, does it resemble more the Lorenz butterfly, or the Rössler attractor?
6. Show that this is the (Lorenz)$/D_1$ quotient map for the Lorenz flow, i.e., that it identifies points related by the π rotation in the (x, y) plane.
7. Show that a periodic orbit of the Lorenz flow in polar representation is either a periodic orbit or a relative periodic orbit (9.13) of the Lorenz flow in the (x, y, z) representation.
8. Show that if a periodic orbit of the polar representation Lorenz is also periodic orbit of the Lorenz flow, their stability eigenvalues are the same. How do the stability eigenvalues of relative periodic orbits of the representations relate to each other?
9. Argue that if the dynamics is invariant under a rational rotation $R_{\pi/m}f(x) = f(\theta + \pi/m)$, a discrete subgroup C_m of $SO(2)$ in the (x, y)-plane, the only non-zero Fourier components of equations of motion are $a_{jm} \neq 0$, $j = 1, 2, \cdots$. The Fourier representation is then the quotient map of the dynamics, $\mathcal{M}/C_m$.

By going to polar coordinates we have quotiented out the π-rotation $(x, y, z) \to (-x, -y, z)$ symmetry of the Lorenz equations, and constructed an explicit representation of the desymmetrized Lorenz flow.

10 What does the volume contraction formula (9.11) look like now? Interpret.

(9.8) **Proto-Lorenz system.** Here we quotient out the D_1 symmetry by constructing an explicit "intensity" representation of the desymmetrized Lorenz flow, following Miranda and Stone [32].

1. Rewrite the Lorenz equation (9.7) in terms of variables

$$(u, v, z) = (x^2 - y^2, 2xy, z)\,. \qquad (9.26)$$

2. Show that this is the (Lorenz)$/D_1$ quotient map for the Lorenz flow, i.e., that it identifies points related by the π rotation (9.8).
3. Show that (9.26) is invertible. Where does the inverse not exist?
4. Compute the equilibria of proto-Lorenz and their stabilities. Compare with the equilibria of the Lorenz flow.
5. Plot the strange attractor both in the original form (9.23) and in the proto-Lorenz for the Lorenz parameter values $\sigma = 10$, $b = 8/3$, $\rho = 28$. Topologically, does it resemble more the Lorenz or the Rössler attractor? For comparison with your plots, you can check Fig. 1 of Ref. [34].
7. Show that a periodic orbit of the proto-Lorenz is either a periodic orbit or a relative periodic orbit of the Lorenz flow.
8. Show that if a periodic orbit of the proto-Lorenz is also periodic orbit of the Lorenz flow, their stability eigenvalues are the same. How do the stability eigenvalues of relative periodic orbits of the Lorenz flow relate to the stability eigenvalues of the proto-Lorenz?
9 What does the volume contraction formula (9.11) look like now? Interpret.
10. Show that the coordinate change (9.26) is the same as rewriting (9.24) in variables $(u, v) = (r^2\cos 2\theta, r^2\sin 2\theta)$, i.e., squaring a complex number $z = x + iy$, $z^2 = u + iv$.

References

[1] P. Cvitanović and B. Eckhardt, "Symmetry decomposition of chaotic dynamics," *Nonlinearity* **6**, 277 (1993).

[2] G. Ott and G. Eilenberger, private communication.

[3] M. Henón and C. Heiles, *J. Astron.* **69**, 73 (1964).

[4] C. Jung and H.J. Scholz, *J. Phys.* **A 20**, 3607 (1987).

[5] C. Jung and P. Richter, *J. Phys.* **A 23**, 2847 (1990).

[6] B. Lauritzen, "Discrete symmetries and the periodic-orbit expansions," *Phys. Rev.* **A 43**, 603 (1991).

[7] B. Eckhardt, G. Hose and E. Pollak, *Phys. Rev.* **A 39**, 3776 (1989).

[8] C. C. Martens, R. L. Waterland, and W. P. Reinhardt, *J. Chem. Phys.* **90**, 2328 (1989).

[9] S.G. Matanyan, G.K. Savvidy, and N.G. Ter-Arutyunyan-Savvidy, *Sov. Phys. JETP 53*, 421 (1981).

[10] A. Carnegie and I. C. Percival, *J. Phys.* **A 17**, 801 (1984).

[11] B. Eckhardt and D. Wintgen, "Symbolic description of periodic orbits for the quadratic Zeeman effect," *J. Phys.* **B 23**, 355 (1990).

[12] J.M. Robbins, "Semiclassical trace formulas in the presence of continuous symmetries," *Phys. Rev.* **A 40**, 2128 (1989).

[13] N. Balasz and A. Voros, *Phys. Rep.* **143**, 109 (1986).

[14] J.M. Robbins, S.C. Creagh and R.G. Littlejohn, *Phys. Rev.* **A39**, 2838 (1989); **A41**, 6052 (1990).

[15] M. Tinkham, *Group Theory and Quantum Mechanics* (McGraw-Hill, New York 1964).

[16] M. Hamermesh, *Group Theory and its Application to Physical Problems* (Addison-Wesley, Reading, 1962).

[17] E.N. Lorenz, "Deterministic nonperiodic flow," *J. Atmos. Sci.* **20**, 130 (1963).

[18] W. Tucker, "The Lorentz attractor exists," *C. R. Acad. Sci. Paris Sér. I Math* **328**, 1197 (1999).

[19] W. Tucker, "A rigorous ODE solver and Smale's 14th problem," *Found. Comput. Math.* **2**, 53 (2002).

[20] M. Viana, "What's new on Lorenz strange attractors?" *Math. Intelligencer* **22**, 6 (2000).

[21] *Universality in Chaos*, P. Cvitanović, ed., (Adam Hilger, Bristol 1989).

[22] Bai-Lin Hao, *Chaos II* (World Scientific, Singapore, 1990).

[23] J. Frøyland, *Chaos and coherence* (Inst. of Phys. Publ., Bristol 1992).

[24] J. Frøyland and K.H. Alfsen, *Phys. Rev. A* **29**, 2928 (1984).

[25] Guckenheimer, J. and Williams, R., "Structural stability of the Lorenz attractor," *Publ. Math. IHES*, vol. 50, pp. 55–72, 1979.

[26] V. S. Afraimovich, B. B. Bykov, and L. P. Shilnikov, "On the appearence and the structure of the Lorenz attractor," *Dokl. Akad. Nauk SSSR* **234**, 336 (1987).

[27] C. Sparrow, *The Lorenz Equations: Bifurcations, Chaos, and Strange Attractors* (Springer-Verlag, Berlin 1982).

[28] Jackson, E. A., *Perspectives of nonlinear dynamics: Vol. 1 and 2.* Cambridge: Cambridge University Press, 1989.

[29] Seydel, R., *From equilibrium to chaos: Practical bifurcation and stability analysis* (Elsevier, New York 1988).

[30] Abraham, R. H. and Shaw, C. D., *Dynamics - The geometry of behavior* (Addison-Wesley, Reading, MA 1992).

[31] M.L. Cartwright and J.E. Littlewood, “On nonlinear differential equations of the second order,” *J. London Math. Soc.* **20**, 180 (1945).

[32] R. Miranda and E. Stone, “The proto-Lorenz system,” ‘*Phys. Letters A* **178**, 105 (1993).

[33] R. Gilmore and C. Letellier, *The Symmetry of Chaos* (Oxford U. Press, Oxford 2007).

[34] C. Letellier, R. Gilmore and T. Jones, “Peeling Bifurcations of Toroidal Chaotic Attractors,” `arXiv:0707.3975v3`.

[35] C. Letellier and R. Gilmore, “Covering dynamical systems: Two-fold covers,” *Phys. Rev. E***63**, 016206 (2001).

[36] R. Gilmore, “Two-parameter families of strange attractors,” *Chaos* **17**, 013104 (2007).

[37] D. A. Cox, J. B. Little, and D. OShea, *Ideals, Varieties and Algorithms* (Springer-Verlag, New York, 1996).